NUWC-NPT TM 942043

NAVAL UNDERSEA WARFARE CENTER DIVISION
NEWPORT, RHODE ISLAND

Technical Memorandum

SUPERCAVITATION DRAG REDUCTION IN HIGH-MACH-NUMBER LIQUID FLOWS

Date: 31 March 1994

Prepared by:

I.N. Kirschner

A.N. Varghese

J.Q. Rice

Advanced Technology and Prototyping Division
Weapons Technology and Undersea Systems Department

LIBRARY USE ONLY

ABSTRACT

A review of supercavitation drag reduction in high-Mach-number liquid flows is presented in order to assess claims that experiments at such high speeds have been performed, and to provide a comparison between the drag of projectiles traveling in water at transonic speeds versus the drag of similar projectiles in air at the same speed.

The physics of high-Mach-number flows are reviewed, including the equations of state in both air and water and the mechanics of shock and expansion waves. A review of literature discussing high-Mach-number supercavitating flows is presented, with a focus on the Nishiyama-Khan model for predicting the drag of supercavitating two-dimensional shapes at subsonic, transonic, and supersonic speeds. The flow in each of these regimes is described, and the drag components are discussed. Based on this background research, estimates of drag coefficients versus Mach number and dimensionalized drag versus speed in both air and water are presented for a wedge.

It is concluded that, contrary to previous speculation, the drag of high-Mach-number projectiles in water is much higher than the drag at the same speed in air. Finally, upgrades to the Nishiyama-Khan model are recommended.

ADMINISTRATIVE INFORMATION

This research was prepared under Job Order Number A99307, "High-Speed Torpedo Hull Performance". The sponsoring activity is the Office of Naval Intelligence, project manager S. Tagg. The authors of this memorandum are located at the Naval Undersea Warfare Center Division, Newport, RI 02841-1708.

ACKNOWLEDGMENTS

The authors wish to thank S. Tagg for his interest in supercavitation drag reduction and his ongoing support of first-principles approaches to problem solving. Thanks to Dr. S. Huyer for reviewing this document.

Reverse Blank

CONTENTS

LIST OF ILLUSTRATIONS

LIST OF TABLES

NOMENCLATURE

A	Surface of integration
$\boldsymbol{B}$	Vector body force per unit mass of fluid in control volume
B	Fluid-specific constant in isentropic relation
$C_D \overset{D}{=} \dfrac{D}{\left(\frac{1}{2}\rho_0 U_0^2\right)(2L\theta)}$	Drag coefficient
c_0	Free-stream sound speed
D	Drag
D_{SH}	Drag contribution from shock system
$d\boldsymbol{A}$	Vector differential area
$\boldsymbol{F}_{SHEAR}$	Total vector shear force exerted on fluid at control surface
g	Acceleration of gravity
h	Fluid-specific enthalpy
L	Characteristic projectile length
$M \overset{D}{=} \dfrac{U_0}{c_0}$	Free-stream Mach number
p	Fluid pressure at a point
p_v	Fluid vapor pressure
Q	Rate of heat transfer to fluid
R	Gas constant
$\mathcal{R} \overset{D}{=} \dfrac{U_0 L}{\nu}$	Free-stream Reynolds number
s	Fluid-specific entropy
$\boldsymbol{U}$	Vector velocity at a point
U	Magnitude of fluid velocity at a point
U_0	Free-stream speed
u	Fluid-specific internal energy
V	Volume of integration
W_{SHEAR}	Rate of work performed on fluid by shear forces on control surface
z	Position in a gravitational field

GREEK LETTERS:

β	Angle of shock with deflected flow direction
γ	Ratio of fluid-specific heats at constant pressure and constant volume
δ	Flow deflection angle (also inexact differential)
ε	Oblique shock-wave angle
θ	Wedge semiangle
μ	Fluid viscosity at a point
ν	Fluid kinematic viscosity at a point
ρ	Fluid density at a point
$\sigma \stackrel{D}{=} \frac{p_0 - p_v}{\frac{1}{2}\rho_0 U_0^2}$	Free-stream cavitation number

SUBSCRIPTS:

0	Indicates free-stream values
1	Indicates values upstream of a shock
2	Indicates values downstream of a shock
AIR	Indicates value in air
MAX AIR	Indicates maximum value in air
MAX WATER	Indicates maximum value in water
t	Indicates partial derivative with respect to time

OTHER MATHEMATICAL SYMBOLS:

$\stackrel{D}{=}$	Defined as
∂	Differential contribution
δ	Inexact differential (also flow deflection angle)
$\frac{D}{Dt}$	Material derivative
∇	Gradient
$\cdot$	Vector inner product

ACRONYMS AND ABBREVIATIONS:

AHSUM	Adaptable High-Speed Undersea Missile
DVE	Discrete Vortex Element
FY	Fiscal Year
NSF	National Science Foundation
NUWC	Naval Undersea Warfare Center

INTRODUCTION

In a recent National Science Foundation (NSF) Symposium on Research Submersibles and Undersea Technologies, a Ukrainian scientist, Viktor Grimchenko, claimed that near-Mach-1 speeds have been achieved in experiments with submerged projectiles (Navy News, 1993). Specifically, it was reported that projectiles consistently exceed speeds of 1000 m/s and that top speeds approaching 1300 m/s have been attained. In order to minimize drag, passive body supercavitation is employed. The experimental facility was described as a 100-m recoil-absorption water tank fitted with a hydrogen gun and a thick steel stopper plate, but no range data was provided.

In response to this claim, NSF chairperson, Dr. Richard Seymour, speculated that supercavitating projectiles traveling at near-Mach-1 speeds in water "may actually have less drag force than at the same speed in air: The density of the cavity is lower than the density of air."

The Naval Undersea Warfare Center (NUWC) Division Newport was tasked with assessing both the claim and the response and expanding the knowledge base concerning supercavitation drag reduction to include high-Mach-number liquid flows. This document presents the requested assessments, along with a description of the physics of high-Mach-number liquid flows, including supercavitation effects.

This work represents a follow-on to a previous effort performed in fiscal year (FY) 1991 (Meng, et al, 1992a, 1992b, 1994). Under that project, a specific vehicle was assessed for the possibility that supercavitation drag reduction was applied for improved performance. Historical and empirical databases were compiled, and a preliminary computational scheme was implemented. The following primary conclusions were drawn.

- Supercavitation drag reduction is the only technique capable of providing the necessary performance improvement for the stated vehicle speed.
- The range of cavitation numbers for which supercavitation occurs is limited to near-zero values (implying shallow depth or extremely high speed).
- Vehicle geometry is important to performance.
- Ventilated cavities and acceleration effects might improve performance.
- A solid-rocket prime mover appears to be the only conventional propulsion system capable of providing the necessary thrust for the stated vehicle speed.
- State-of-the-art rockets can provide the required thrust, energy density, and power densities.
- Rocket-motor performance is depth-dependent.

The current effort also complements ongoing development of the adaptable high-speed undersea missile (AHSUM). NUWC has been investing in such research since 1978. The

program has been supported by PDA Engineering of Costa Mesa, California since 1987. Two missile concepts are under consideration for close-in, quick-response kinetic target kill, (1993).

One of the concepts employs supercavitation drag reduction to achieve the required speeds. Drag coefficients that are at least one order of magnitude less than that of the current fleet torpedo have been achieved in experiments. A mid-range land-based test is about to be performed in which it is planned to penetrate targets of interest at speeds exceeding 820 m/s, with a predicted drag coefficient roughly two orders of magnitude less than that of the current fleet torpedo (Kochendorfer, 1993). As part of this project, a target-to-launch design approach that allows systematic specification of most key system parameters based on the target kinetic-penetration characteristics has been developed (Kirschner, (1993).

A rocket-propelled supercavitating AHSUM variant is shown in figure 1. This vehicle is roughly 38 cm long. Stability is provided by cavity-riding fins consisting of plate springs with special trailing-edge treatment in conjunction with a carefully chosen nose profile. These vehicles have been tested at speeds exceeding 180 m/s in a 5-m water tank.

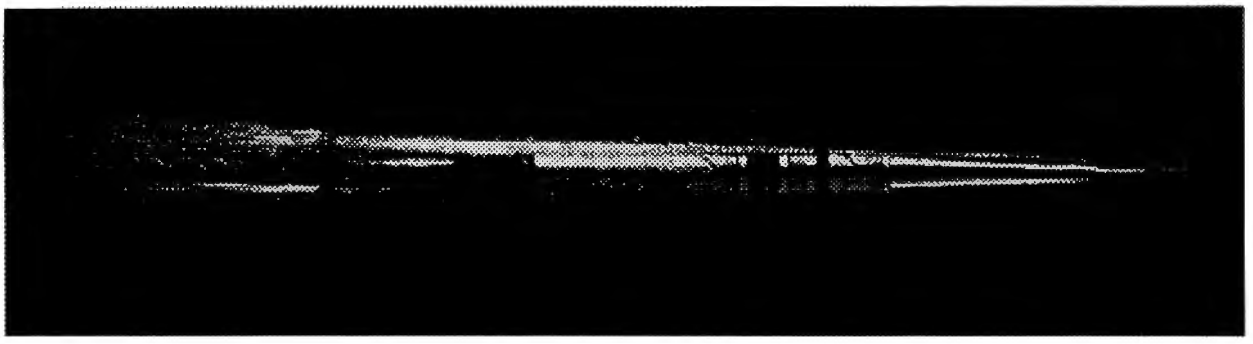

Figure 1. Supercavitating Rocket-Propelled AHSUM Variant Flying at 180 m/s Underwater

HIGH-MACH-NUMBER FLOWS

The sound speed in fresh water at 25°C is 1497 m/s, while in air the sound speed is 343 m/s at 20°C. The ratio of free-stream velocity, U_0, to free-stream sound speed, c_0, is known as the free-stream Mach number:

$$M \stackrel{D}{=} \frac{U_0}{c_0}.$$

Because of the relatively high drag of projectiles traveling in water, along with the large value of the sound speed, practical projectile performance is usually limited to very low Mach numbers.

Under certain conditions, projectile drag in water can be significantly reduced by employing passive body supercavitation. As the speed of a submerged body increases, the minimum pressure on the body surface decreases. At high-enough speeds the minimum pressure drops to the liquid vapor pressure,and the fluid in the region of low pressure cavitates at constant temperature to the vapor phase. The density, ρ, viscosity, μ, and kinematic viscosity, ν, of the fluid in the vapor cavity are greatly reduced, as are wall shear stresses. If the body is designed to take advantage of the reduced skin friction, significant drag reduction can be achieved. The quantity characterizing the conditions under which cavitation occurs is the *cavitation number*, σ, defined as

$$\sigma \stackrel{D}{=} \frac{p_0 - p_v}{\frac{1}{2}\rho_0 U_0^2},$$

where p is the pressure, p_v is the vapor pressure of the ambient fluid (that is, the pressure below which the liquid cavitates to form a vapor), and the subscript 0 indicates conditions in the free-stream.

As the drag is reduced, projectiles can travel at higher speeds for longer ranges. The upcoming AHSUM tests will take place at a muzzle velocity of over 820 m/s; the corresponding Mach number is 0.55. There is no reason to believe that much higher speeds cannot be attained. If the Grimchenko claim is correct, the Ukrainians have succeeded in achieving a Mach number of 0.87. Under such conditions, the compressibility of the liquid becomes important, eliminating one of the convenient assumptions made in predicting low-Mach-number liquid flows.

There are three Mach-number regimes of interest:

1. Subsonic, heuristically defined as the regime in which the relative velocity at all points in the fluid is less than the sound speed;
2. Transonic, in which the local velocity at some points exceeds the sound speed and a detached bow shock forms; and,
3. Supersonic, in which the bow shock becomes attached.

More precise definitions of these regimes will be given below.

Governing Equations of Motion for Compressible Fluid Flows

The equations of motion of a compressible fluid express the conservation of mass and momentum and energy of the flow, along with a form of the second law of thermodynamics. These relationships, as derived in Zucrow and Hoffman (1976), are stated in table 1 in both integral and differential form. (Nomenclature is defined on page v.)

These equations, supplemented with an equation of state relating the fluid properties, describe the motion of the fluid. When boundary conditions on the body surface are imposed, a solution of the boundary-value problem can be found. Such solutions are often approximated numerically. Various simplifications have been developed for special cases, reducing the complexity of the boundary-value problem and allowing a more economical solution.

Table 1. Equations of Motion for a Compressible Fluid

EQUATION	INTEGRAL FORM	DIFFERENTIAL FORM
Continuity	$\int_V \rho_t \, dV + \int_A \rho \boldsymbol{U} \cdot d\boldsymbol{A} = 0$	$\rho_t + \nabla \cdot (\rho \boldsymbol{U}) = 0$
Momentum	$\int_V \boldsymbol{B}\rho \, dV - \int_A p \, d\boldsymbol{A} + \boldsymbol{F}_{SHEAR} = \int_V (\rho \boldsymbol{U})_t \, dV + \int_A \boldsymbol{U}(\rho \boldsymbol{U} \cdot d\boldsymbol{A})$	$\rho \frac{D\boldsymbol{U}}{Dt} + \nabla p - \rho \boldsymbol{B} - d\boldsymbol{F}_{SHEAR} = \boldsymbol{0}$
Energy	$\dot{W}_{SHEAR} - \dot{Q} + \int_V \frac{\partial}{\partial t}\left[\rho\left(u + \frac{U^2}{2} + gz\right)\right] dV + \int_A \left(h + \frac{U^2}{2} + gz\right)(\rho \boldsymbol{U} \cdot d\boldsymbol{A}) = 0$	$\partial \dot{W}_{SHEAR} - \partial \dot{Q} + \rho \frac{D}{Dt}\left(h + \frac{U^2}{2} + gz\right) - p_t = 0$
Entropy	$\int_V (s\rho)_t \, dV + \int_A s(\rho \boldsymbol{U} \cdot d\boldsymbol{A}) \geq \frac{\dot{Q}}{t}$	$\rho \frac{Ds}{Dt} \geq \frac{\partial \dot{Q}}{t}$

Equations of State for Air and Water

The familiar gas laws relating density, pressure, and temperature do not apply to compressed liquids. For water, Tait's equation (Nishiyama and Khan, 1981a, 1981b) is an acceptable approximation. The equations of state for air and water are provided in table 2. The quantity γ is the ratio of the fluid-specific heat at constant pressure to that at constant volume. T is the temperature, R is the gas constant for air, while the constant B is a fluid property with units of pressure (Nishiyama and Khan, 1981a, 1981b) in units of mass per unit area.

Figure 2 shows the variation in pressure with density based on the isentropic relation for air and Tait's isentropic relation for water. It can be seen that, for water, a small variation in density is associated with a tremendous variation in pressure relative to air.

Table 2. Equations of State for Air and Water

AIR	
Ideal Gas Law Approximation	$\frac{p}{\rho} = RT$
Isentropic Relation	$\frac{p+B}{\rho^{\gamma}} = \text{CONSTANT};$ $\gamma = 1.40,\ B = 0$
WATER	
Tait's Isentropic Relation	$\frac{p+B}{\rho^{\gamma}} = \text{CONSTANT};$ $\gamma = 7.15,\ B = 3000\ \text{kg/m}^2$

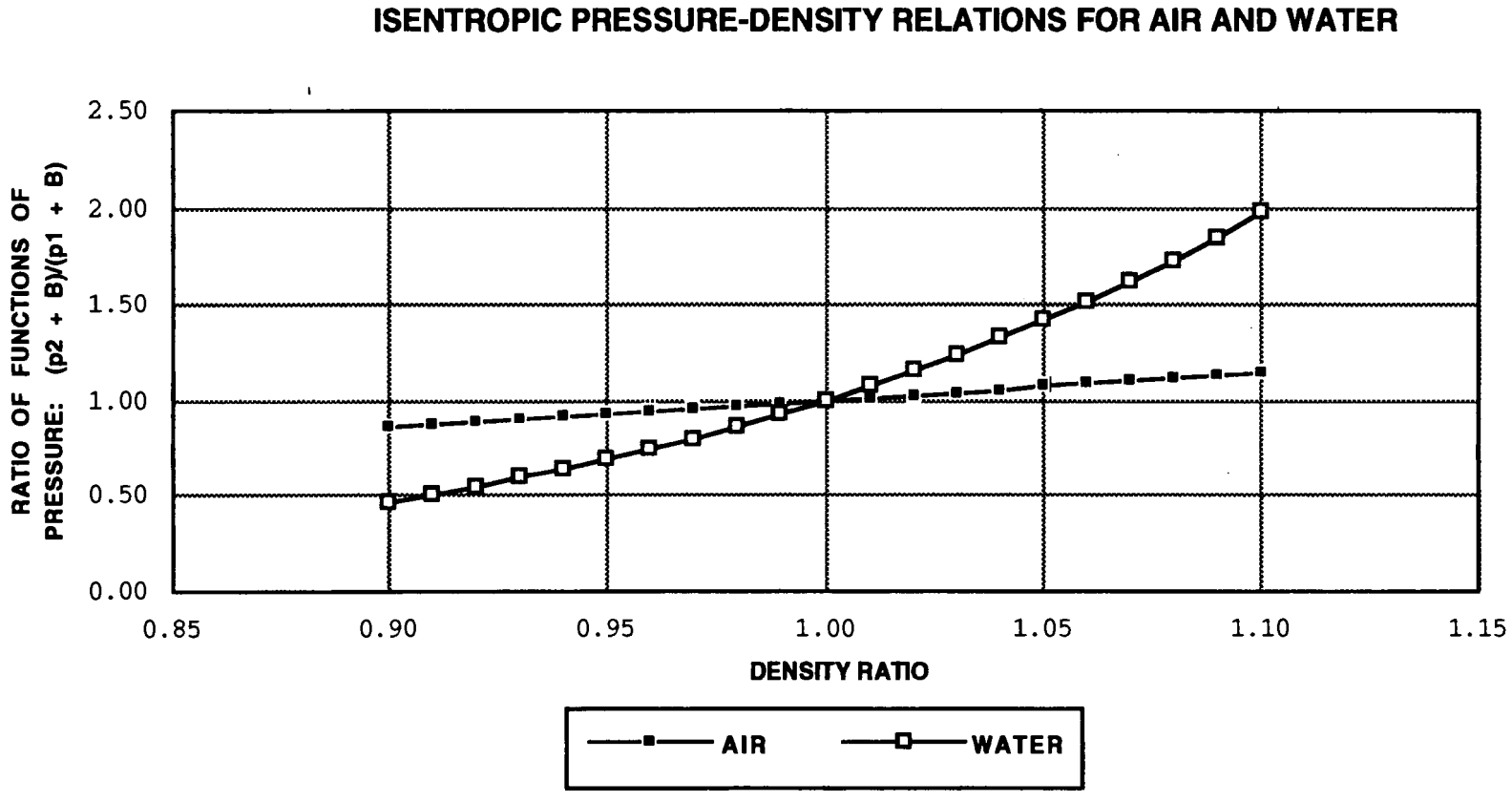

Figure 2. Variation of Pressure with Density

Shock- and Expansion-Wave Mechanics for Perfect Gases

Under certain conditions, including transonic and supersonic flow past a body, a compressible fluid can experience an abrupt change of state. As described in Zucrow and Hoffman (1976), this takes place on a very steep wave front across which the pressure rises drastically. Such waves are called *shock waves*. In steady flow, shock waves travel with the body. The pressure rise is accompanied by an increase in density. Since the sound speed is a state-dependent fluid property, it usually changes across the shock.

In changing state across the shock wave, the fluid is subject to an irreversible process (that is, the useful energy of the fluid decreases as the shock is traversed). The energy for compressing the gas is derived from the kinetic energy of the fluid before it reaches the shock wave. The kinetic energy downstream is less than it would be if the fluid were compressed isentropically. This energy is converted to thermal energy and is associated with increased entropy and a static temperature greater than that associated with isentropic compression.

Shock waves are classified according to the orientation of the wave front with respect to the flow direction. Those oriented perpendicularly to the flow are called *normal shocks*, while those forming an oblique angle with the flow are termed *oblique shocks.*

The change of state across a shock wave is so rapid that its width is often negligible compared to other dimensions characterizing the flow. The theory of such shock waves in both perfect and imperfect gases is well developed. More detailed structure of finite-width shocks can be determined numerically.

An excellent overview of shock-wave theory is provided in Zucrow and Hoffman (1976). The traditional development begins with the theory of normal shocks as deduced from one-dimensional flow considerations. These results are then extended to oblique shocks by analysis of the normal and tangential velocity components just upstream and just downstream of the wave front.

A stationary one-dimensional normal shock wave is schematized in figure 3. Just upstream of the shock, the Mach number is greater than unity. As the flow traverses the shock wave, the pressure increases and the velocity decreases. It can be shown that the Mach number downstream of the normal shock wave is always less than unity. Another result of this theory is that, for weak shocks, the entropy increase is insignificant

Figure 4 shows representative flow cases for attached and detached oblique shock waves. It can be shown that the velocity component tangential to the front remains unchanged across the shock; while the normal velocity component satisfies the same relationships as the flow across a normal shock.

Oblique shocks are associated with a concave deflection of the flow. The other case, flow past a convex corner, is depicted in figure 5. The flow discontinuity associated with the required expansion of flow around the corner is termed an *expansion wave*. Certain types of expansion waves (called *simple waves* or *Prandtl-Meyer waves*) can be analyzed by one-dimensional techniques. In such flows, it can be shown that the velocity increases and the pressure decreases as the fluid traverses the *expansion fan*.

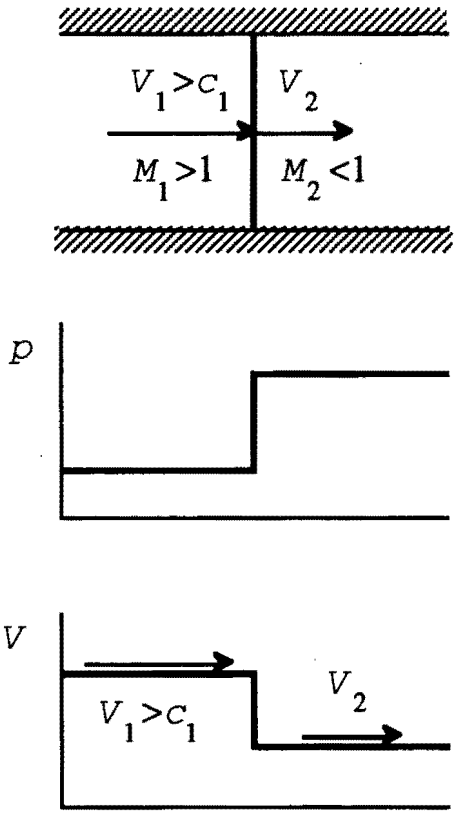

Figure 3. Schematic of a One-Dimensional Normal Shock Wave

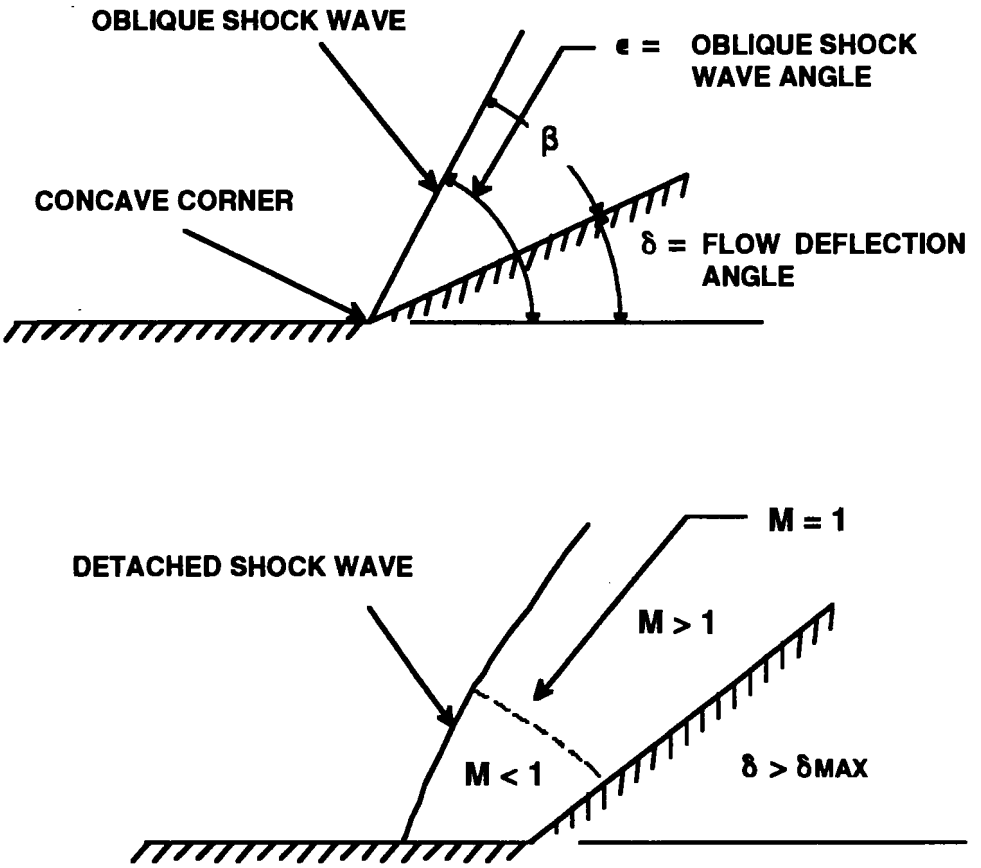

Figure 4. Schematics of Attached and Detached Oblique Shocks

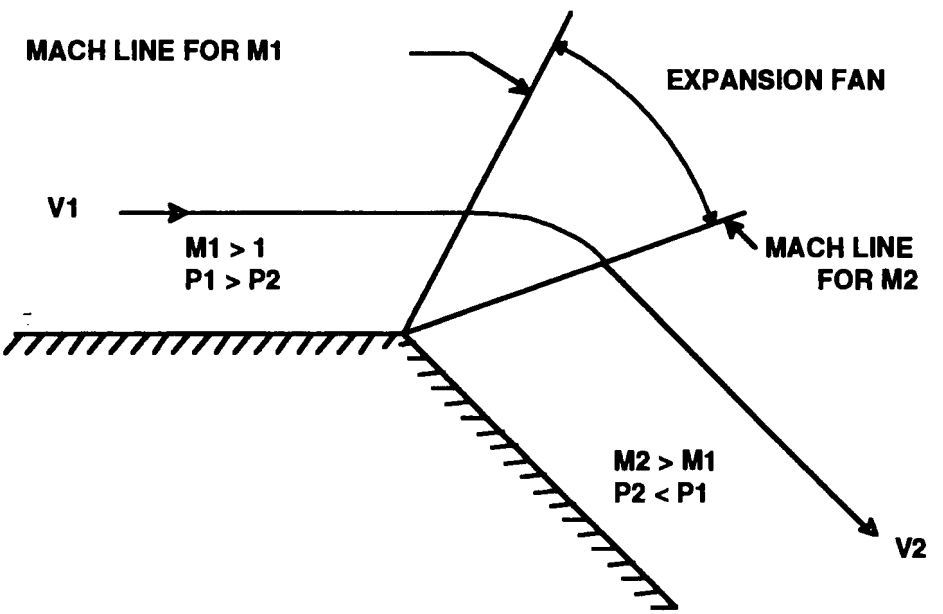

Figure 5. Schematic of an Expansion Wave

Shock-Wave Drag

Downstream of a shock wave the fluid pressure expands isentropically. Far downstream of a shock system, the fluid static pressure attains the same value as that far upstream of the shock system. However, because of the conversion of kinetic energy to thermal energy across the shock, the velocity behind the shock system does not return to the free-stream condition. The steady-flow situation is depicted in figure 6 with a body-fixed inertial reference system.

The momentum equation (table 1) can be used to show that, even in frictionless flow (for which shear forces are zero), there must be a pressure force acting on the body in the flow direction. This drag force is termed *shock- wave drag*. It must be accounted for in predicting the total vehicle drag.

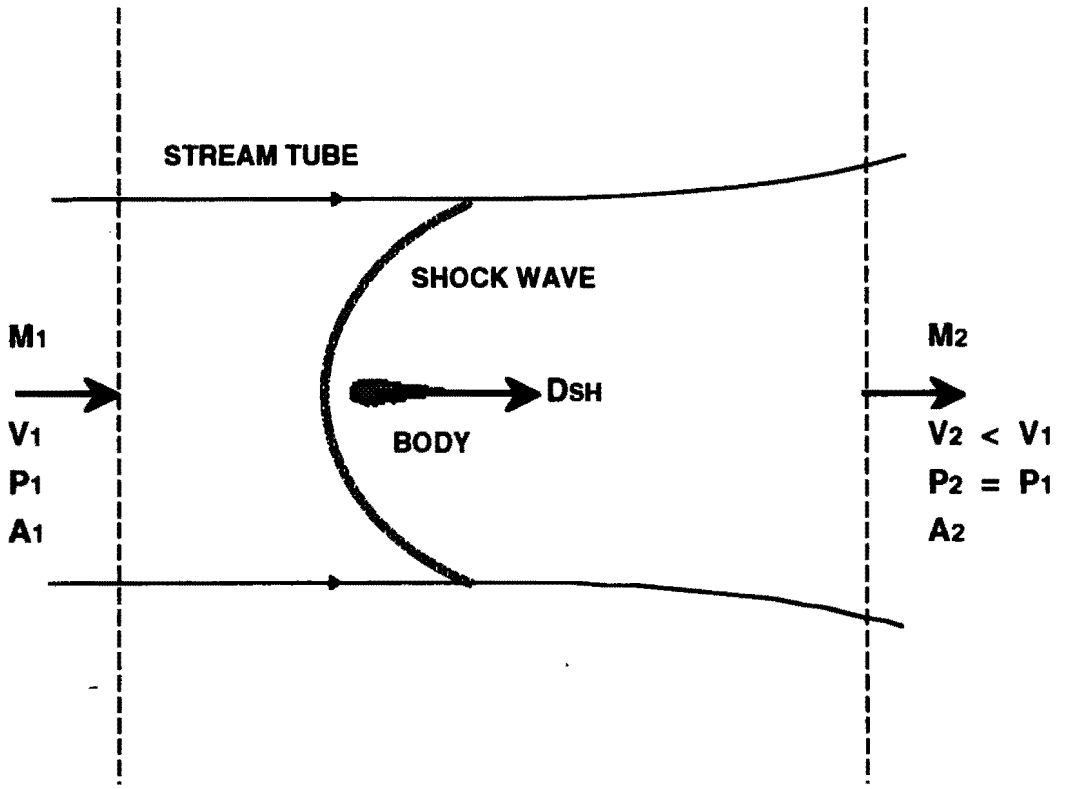

Figure 6. Flow Diagram for Analyzing Shock-Wave Drag

LOW-MACH-NUMBER SUPERCAVITATING FLOWS

Low-Mach-number supercavitating flows were discussed in the documentation associated with the vehicle assessment mentioned in the introduction. Cavitation theory has been widely studied, and many excellent references,notably Newman (1980), are available. Only a brief description will be given here.

The classical approach to the investigation of cavitation in low-Mach-number flows is an extension of the theory of incompressible ideal flow. With L a length scale characterizing the flow, the Reynolds number is defined as

$$\mathcal{R} \stackrel{\text{D}}{=} \frac{U_0 L}{\nu}.$$

As the Reynolds number increases, the effects of viscosity in attached noncavitating flow become increasingly confined to the boundary layer, which approximately conforms to the body surface. If the flow outside the boundary layer and any separation or cavitation regions is both incompressible and irrotational, the flow is termed *ideal*, and it can be shown that a *velocity potential* exists. The governing equation of motion for the resulting boundary-value problem is Laplace's equation. The boundary conditions on velocity potential for flow past a rigid impermeable body are purely kinematic and of the Neumann type.

For any known steady velocity field, pressure can be determined by integrating the momentum equation along a streamline from a point where all conditions are known. The resulting equation is of the Bernoulli type. For ideal flow with well-posed boundary conditions, the velocity field can be computed from the solution of the boundary-value problem for the velocity potential. Bernoulli's equation for ideal flow is quite simple, and the computation of pressure is straightforward, once the velocity field has been determined.

In the prediction of cavitating flow fields, advection through the cavity boundary is zero, providing a kinematic condition on the flow outside the cavity. However, the cavity shape is not known *a priori*, and another condition is required to solve the boundary-value problem. Within the vapor cavity, where the flow is not necessarily ideal, the relative magnitudes of the terms of the momentum equation indicate that the pressure is nearly constant, with a value equal to the vapor pressure of the fluid. Thus, for purposes of predicting the cavity shape, the pressure along the cavity streamline is usually taken as equal to the vapor pressure, providing a dynamic condition.

In general, the resulting boundary-value problem is nonlinear. Under certain conditions (for example, for thin bodies in two-dimensional flow or slender bodies in axisymmetric flow) simplifications can be made that eliminate the nonlinearity. For more complicated cases, an iterative approach,wherein the cavity geometry is modified until both the kinematic and dynamic conditions on the cavity streamline are satisfied, is often employed.

In all of these classical approaches, a cavity closure condition must also be specified in order to determine a unique solution. In order to determine the cavity detachment point from smooth bodies, cavity detachment conditions must be specified as well. A relevant overview of such a procedure is provided in Vorus (1986 and 1991), the second reference of which was generated as part of the FY 91 vehicle assessment effort.

HIGH-MACH-NUMBER SUPERCAVITATING FLOWS

Thus, for low-Mach-number-, high-Reynolds-number-cavitating flows of interest in the design and analysis of high-speed submerged vehicles, a well-developed theory exists that allows determination of the velocity field through solution of Laplace's equation, which is elliptic. For high-Mach-number flows, however, the governing equation is hyperbolic. Most of the work in high-Mach-number flows has dealt with gas dynamics, for example, high-speed air flow past aircraft.

Because the relatively high drag of submerged projectiles and the large value of the sound speed in water have made high-Mach-number undersea projectiles impractical for traditional applications, high-Mach-number liquid flows have not been extensively studied. High-Mach-number supercavitating flows are rarely discussed.

A literature search was performed during the course of the current effort. Noteworthy citations are listed in the bibliography. Table 3 is a summary of the relevant physics addressed by the various authors. The most useful references for the current effort were two papers published in the Bulletin of the Japanese Society of Mechanical Engineers (T. Nishiyama and O.F. Khan, 1981a, 1981b). These are discussed in more detail below. Other useful sources of information were standard texts concerning compressible flow, especially those by Zucrow and Hoffman (1976) and Pai and Shijun (1991).

Table 3. Physics Addressed in Various References

SOURCE	WETTED DRAG	CAVITATION EFFECTS	MACH EFFECTS	HIGH-MACH-NUMBER SUPERCAVITATION EFFECTS
Ashley and Landahl	√		√	
Chou	√	√		
Hickox, et al	√	√		
Hirt		√		
Hoerner	√	√	√	
Oberkampf and Wolfe	√	√		
Pai and Shijun		√	√	
Shapiro	√		√	
Streeter	√	√	√	
Sutton			√	
Nishiyama and Khan				√
Van Dyke	√	√	√	
Vorus	√	√		
Wu		√		

The Nishiyama-Khan Model

The references by Nishiyama and Khan (1981a and 1981b) describe the theory of two-dimensional high-Mach-number subsonic, transonic, and supersonic cavitating liquid flows. Their research represents an extension of the study of steady high-Mach-number gas flows past double wedges. Wedges are of particular interest in the study of compressible flow because they are geometrically simple, yet contain the three primary structures of interest: normal and oblique shock waves and expansion waves.

The mathematical development of the Nishiyama-Khan model is well presented in terms of standard compressible-flow theory and will not be repeated here. An overview can be summarized as follows.

- It is shown in the Nishiyama-Khan references that the flow is approximately isentropic for density variations up to about 10 percent from free-stream values. Tait's isentropic relation is identified as the proper equation of state in water.
- As in the theory of high-Mach-number gas flows past bodies, two critical Mach numbers are identified --a lower and an upper-- that delimit the transonic regime. The lower critical Mach number is defined as that lowest subsonic free-stream Mach number at which the local sonic velocity first occurs on the body surface. The upper critical Mach number is defined as that supersonic free-stream Mach number at which the region of local subsonic flow downstream of the oblique bow shock first disappears.
- Selectively neglecting products of perturbation velocities and their derivatives, Nishiyama and Khan derive a single nonlinear equation for the velocity potential valid for all three flow regimes.
- For subsonic flow, *local linearization* is used to reduce the problem to the standard elliptic incompressible flow problem. This represents an extension of the well-known Prandtl-Glauert transformation.
- For transonic flow, which is a problem of the mixed type, it is necessary to assume that the velocity behind each shock wave can be neglected. Local linearization and the method of Sprieter (1957) are then applied, resulting in an integral for the perturbation velocity that depends solely on the wedge geometry.
- For supersonic flow, a very simple solution for the perturbation velocity results because of the simplifications inherent in boundary-value problems of the purely hyperbolic type.

Results of the technique are also provided in the two Nishiyama-Khan references. Figure 7 presents a schematic of each two-dimensional flow regime for a wedge, supplemented with the cases of fully wetted- and in-air flow. These diagrams show the primary details of the flow structure as predicted by the Nishiyama-Khan model. Note that there are other flow structures

(such as a turbulent boundary layer and an assumedly complicated flow in the region of cavity closure) that are not predicted by the model.

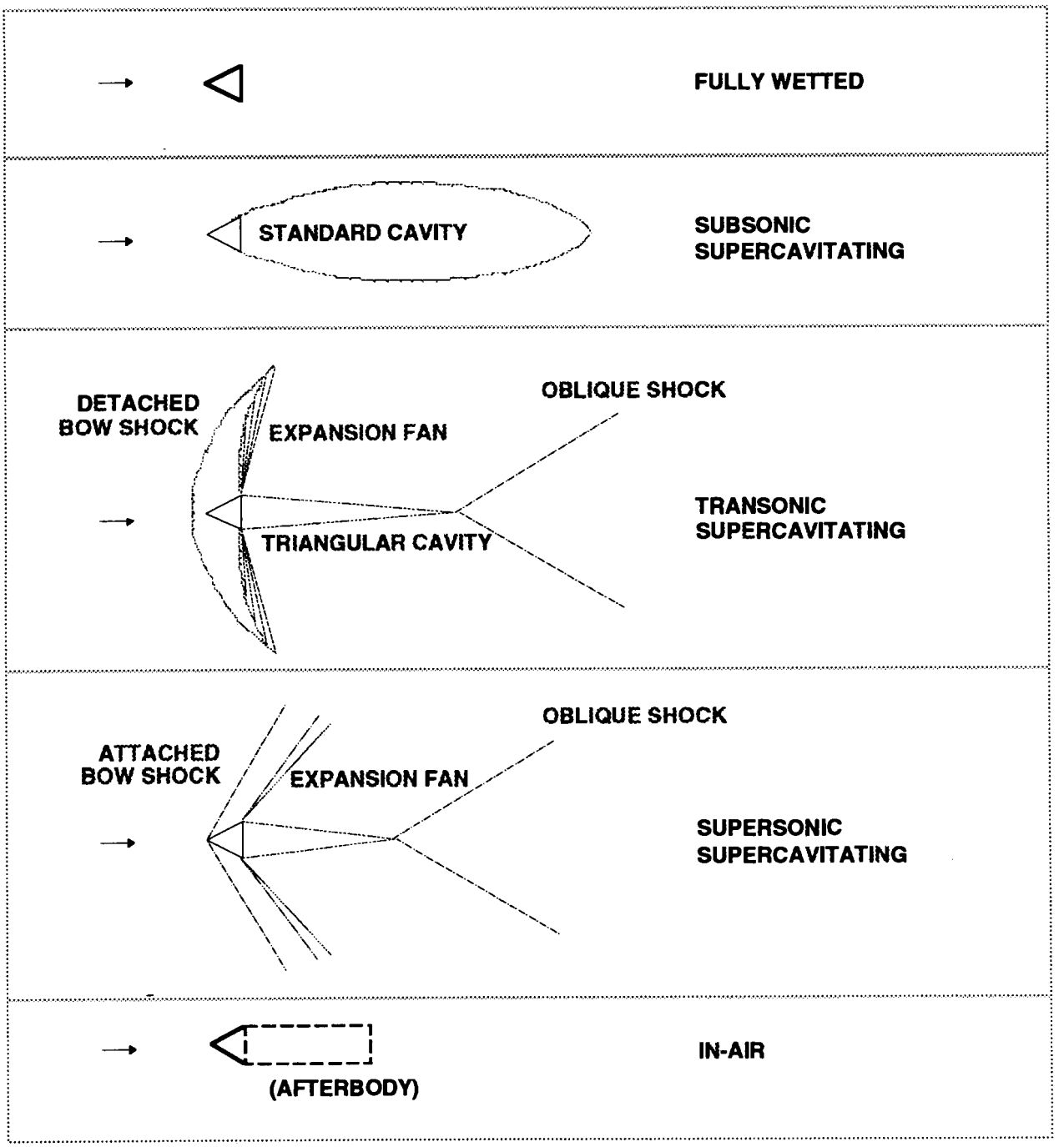

Figure 7. Menu of Flow Regimes

Depending on the Reynolds number, fully wetted flow involves a separation bubble behind the body (not shown on the figure, but having roughly the same shape as the cavity in the second case). Subsonic supercavitating flow is characterized by a vapor cavity as shown.

In transonic supercavitating flow, a detached bow shock wave forms, followed downstream by a Prandtl-Meyer expansion fan originating at the wedge shoulder. The flow is subsonic downstream of the bow shock, increases to sonic speed on the sonic line (which delimits the upstream extent of the expansion fan), and accelerates to supersonic speed through the expansion. The cavity shape is triangular. The flow decelerates to subsonic speed as it passes through the oblique shock originating at the cavity trailing edge.

In supersonic supercavitating flow, the bow shock is attached at the wedge apex. There is no sonic line since the flow speed is supersonic everywhere in the field. Similar to the transonic case, the cavity shape is triangular, a Prandtl-Meyer expansion fan originates at the wedge shoulder, and an oblique shock occurs at the cavity trailing edge.

At low-Mach numbers, the in-air case resembles the fully wetted flow, with separation occurring behind the body, depending on the Reynolds number. Since the ambient fluid is already in a gaseous state, no cavity can form. At high-Mach numbers, however, a shock wave system can form, consisting of a bow shock (detached in the transonic case and attached in the supersonic case) and an expansion fan at the wedge shoulder. The interaction between the separation bubble and the shock system is complicated and can result in an oblique shock at the bubble trailing edge. The notional afterbody depicted in dashed lines for the in-air case is discussed in the next section.

Nishiyama and Khan provide expressions for surface velocity, surface pressure, cavity shape, and cavity drag for a family of symmetrical single-wedge shapes. Due to the difficulty of performing experiments in water at high-Mach numbers, empirical data is sparse. However, some validation in the subsonic regime is provided, and comparison with other solution techniques lends credence to their results. The key trends, detailed in Nishiyama and Khan (1981a and 1981b) relating drag, cavity length, and surface velocity and pressure to Mach and cavitation number can be summarized as follows.

- It is interesting to note that, in the transonic and supersonic regimes, the predicted cavity profile is triangular.
- The bow shock is detached at lower values of the Mach number. It weakens and becomes more oblique downstream, asymptoting to a free-stream Mach wave. With increasing free-stream Mach number, the detached bow shock moves closer to the wedge apex and weakens, until, at the upper critical Mach number, it becomes attached.
- In the transonic regime the flow decelerates discontinuously to subsonic speed through the bow shock, accelerates continuously to sonic speed on the *sonic line*, then accelerates to supersonic speed through an expansion fan that originates at the wedge

shoulder. At speeds greater than the upper critical Mach number, the flow between the bow shock and the expansion fan is no longer subsonic.

- In transonic and supersonic flow, the fluid is subject to an abrupt turn through the expansion fan originating at the wedge shoulder, which results in a triangular-shaped cavity profile. Flow deflection at the wedge shoulder increases with an increase in either Mach or cavitation numbers.
- In subsonic flow, the cavity length increases with increasing Mach number, as does the cavity drag coefficient, especially above Mach numbers of 0.6. In transonic and supersonic flow, the cavity length decreases with increasing Mach number.
- At transonic speeds, the surface pressure coefficient, which varies along the wedge, increases with increasing Mach number. At supersonic speeds, the surface pressure coefficient, which is constant along wedge, decreases with increasing Mach number. In both cases, the pressure coefficient increases with increasing cavitation number.
- The cavity drag coefficient increases sharply with increasing Mach number in the transonic regime. It decreases discontinuously as the Mach number increases incrementally through the upper critical Mach number. In the supersonic regime, it decreases with increasing Mach number.

DRAG PHYSICS

The total drag on a body in any of the flow regimes shown in figure 7 has two components: a skin-friction component (equal to the integral over the body surface of the axial component of the shear stress) and a pressure component (equal to the integral of the axial component of the differential pressure force). In the fully wetted case, the relative importance of these two components is very dependent on the Reynolds number. At very low Reynolds numbers, separation is limited to two weak vortex systems located very close to the wedge shoulders. In that case, almost complete pressure recovery occurs on the downstream face of the wedge, and the skin-friction drag component dominates. As the Reynolds number is increased, separation is more extensive and pressure drag becomes increasingly important.

In the high-speed cases of interest, the pressure drag dominates. After cavitation occurs, the pressure on the downstream face of the wedge is always nearly that of the vapor pressure of the ambient fluid; stagnation pressure is never recovered. Thus *cavity drag* begins to dominate skin-friction drag. At high Mach numbers, the pressure drag is increased by the wave drag associated with the shock system, as discussed above. At such high speeds, the pressure drag is so high that skin friction is justifiably neglected. In the Nishiyama-Khan model, cavity and shock-wave drag are reported as a single quantity.

In low-Mach-number supercavitating flows, although the nose geometry is extremely important to cavitation inception, the cavity shape is almost unaffected by the geometry of the body within the cavity. From momentum considerations, it can be shown that the cavity must be convex. For many bodies of interest, this results in a cavity that continues to increase in transverse dimensions downstream of the cavity detachment point. Thus, if the shape of the cavity can be accurately predicted, the designer has the freedom to choose the shape of the afterbody within the cavity to optimum advantage. That is, the afterbody can be designed to nearly "fill up" the cavity, increasing the usable volume without significantly increasing the drag.

Supercavitation-drag reduction often seems particularly effective at low-Mach numbers because drag coefficients for submerged vehicles are usually made dimensionless with respect to the vehicle axial projected area. As predictions of cavity shape become more accurate, designers can allow the maximum sectional area of the vehicle to approach that of the cavity, reducing the drag coefficient. While the total drag of the vehicle has not changed, more effective use has been made of the volume within the cavity. Thus, the drag coefficient based on axial projected area is a useful figure of merit for this aspect of the design process.

For transonic or supersonic supercavitating flow past a two-dimensional wedge, however, the Nishiyama-Khan theory predicts that the cavity is triangular, with its apex pointing downstream. Thus, although use can be made of this volume, the maximum transverse dimension can never

exceed the base dimension of the wedge. In such cases supercavitation provides less drag reduction than in the low-Mach-number case, although the vehicle volume could be increased somewhat within the cavity.

An even more perplexing question is raised by the prediction of the triangular-shaped cavity behind a wedge in transonic and supersonic flow. Consider a body such as that represented by the in-air case (figure 7), that is, with a notional rectangular afterbody extending straight downstream from the base of the wedge-shaped nose. At high-Reynolds numbers and at low Mach numbers *in air*, a separation bubble will form the length of which is Reynolds-number dependent. However, over a wide range of Reynolds numbers, skin friction on the afterbody will substantially increase the total drag of the body. At high Mach numbers, however, a shock system will form similar to that described above, consisting of a bow shock, an expansion fan at the wedge shoulder, another expansion fat at the afterbody trailing edge, and (probably) an oblique shock wave originating at the trailing edge of the separation bubble behind the afterbody. *In water*, however, a vapor cavity will form at the wedge shoulder for any case in which the local pressure drops below the vapor pressure of the ambient fluid. According to the Nishiyama-Khan model, however, the cavity streamline is straight, since the governing equation of motion is hyperbolic. How does such a cavity close?

Supercavitating Vice In-Air Drag

Although that question indicates a need for additional understanding of the interaction between cavitation- and compressibility effects in high-Mach-number liquid flows, insight concerning Dr. Seymour's speculation that supercavitating projectiles traveling at near-Mach-1 speeds in water "may actually have less drag force than at the same speed in air" can be gleaned by direct comparison of the pressure drag as predicted by the Nishiyama-Khan model with the drag at high-speed in air.

A summary of the drag contributions in the two cases is listed in table 4. Reduced skin friction in the supercavitating case only occurs if an afterbody exists within the cavity. Such is not the case for a wedge.

The quantities reflecting Dr. Seymour's association of the presumed drag reduction for the in-water supercavitating case with the difference in density between water vapor and air are listed in table 5. Indeed, the density of water vapor under the conditions indicated is only 1 percent that of air. Thus, if drag were proportional to the density of the fluid in contact with the body, the drag in air would greatly exceed that in water. However, such is not the case.

Table 4. Supercavitating- Vice In-Air Drag at High-Mach Numbers

SUPERCAVITATING CASE	IN-AIR CASE
Reduced skin friction associated with low-cavity velocities, density, and viscosity	Full skin friction
Base drag	Separation drag
Mach-number effects	Mach-number effects

Table 5. Densities of Air, Water, and Vapor

FLUID	DENSITY	DENSITY RATIO WITH AIR
	(kg/m^3)	
Air[1]	1.2318	1
Water[2]	999.55	811
Vapor[3]	0.0133	0.01

1 288.7 K 101.35 kPa
2 288.7 K 101.35 kPa
3 288.7 K 1.72 kPa

An accurate prediction of the drag in each case must account for all contributions to pressure drag and skin-friction drag. As reported in table 4, Mach-number effects are important in both cases.

Estimates of Drag in Water and in Air

The Nishiyama-Khan model was used to compute the drag coefficient (neglecting the contribution from skin friction, which is insignificant at these speeds) at various Mach numbers above the lower critical Mach number for flow past a two-dimensional symmetrical wedge of apex semi-angle $5.7°$ at cavitation numbers of σ=0.05, 0.20, and 0.45. The drag coefficient is made dimensionless with respect to the free-stream dynamic pressure of the ambient fluid and the total base dimension of the thin wedge:

$$C_D \stackrel{D}{=} \frac{D}{\left(\frac{1}{2}\rho_0 U_0^2\right)(2L\theta)},$$

where dimensions are indicated in figure 8 and D is the drag per unit-length of the two-dimensional wedge.

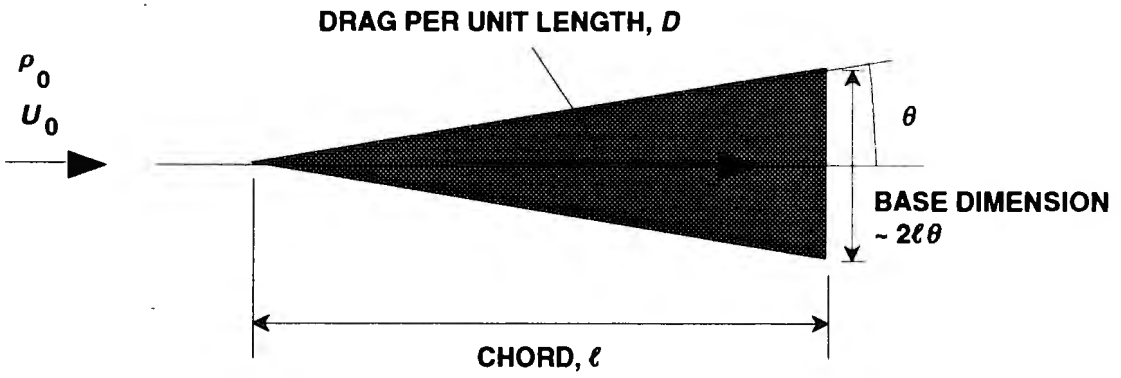

Figure 8. Wedge Non-Dimensionalization

The results of the drag prediction for the supercavitating wedge using the Nishiyama-Khan model are plotted in figure 9, along with empirical values for in-air flow past the same wedge from Hoerner (1965). A theory for drag prediction at high-Mach number in air is reported in Ashley and Landahl (1965).

The maximum in-air drag coefficient is greater than that for the supercavitating case in water, even at the highest value of cavitation number for which the computation was performed. The maximum drag coefficient in air is $C_{D\text{MAX AIR}} \cong 1.2$, while that in water is $C_{D\text{MAX WATER}} \cong 0.9$, 0.7, and 0.4 at $\sigma = 0.05, 0.20,$ and $0.45,$, respectively.

To assess Dr. Seymour's speculation, dimensional drag data were computed using this definition. The results are plotted in log-log format in figure 10 for a $5.7°$ wedge of chord length 1 meter traveling in water of density $998 kg/m^3$ and in air of density $1.2 kg/m^3$. It can be seen that, over the range of data plotted for each case, the drag in water is three to four orders of magnitude higher than that in air.

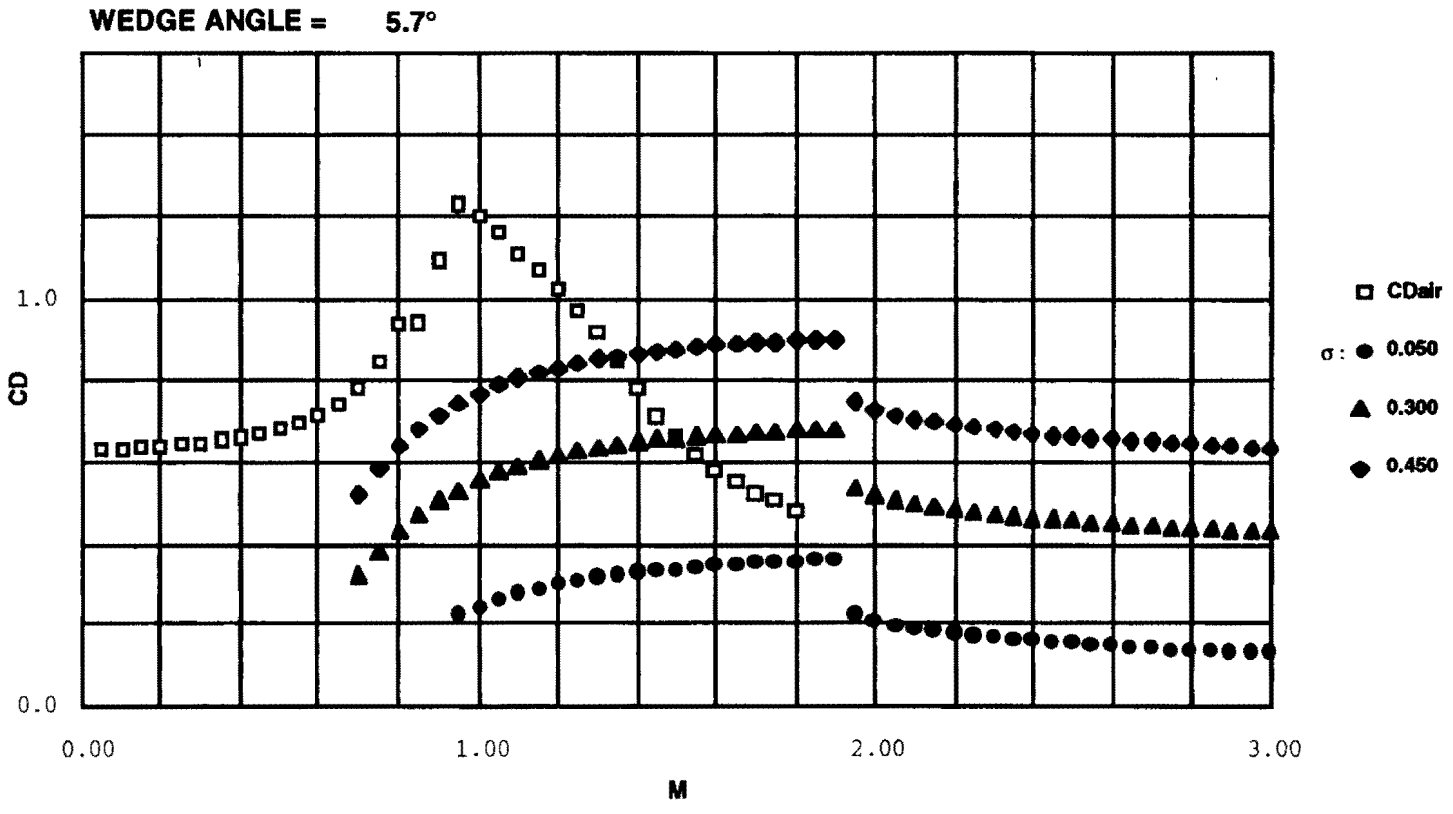

Figure 9. Estimates of Drag Coefficients in Air and Supercavitating in Water

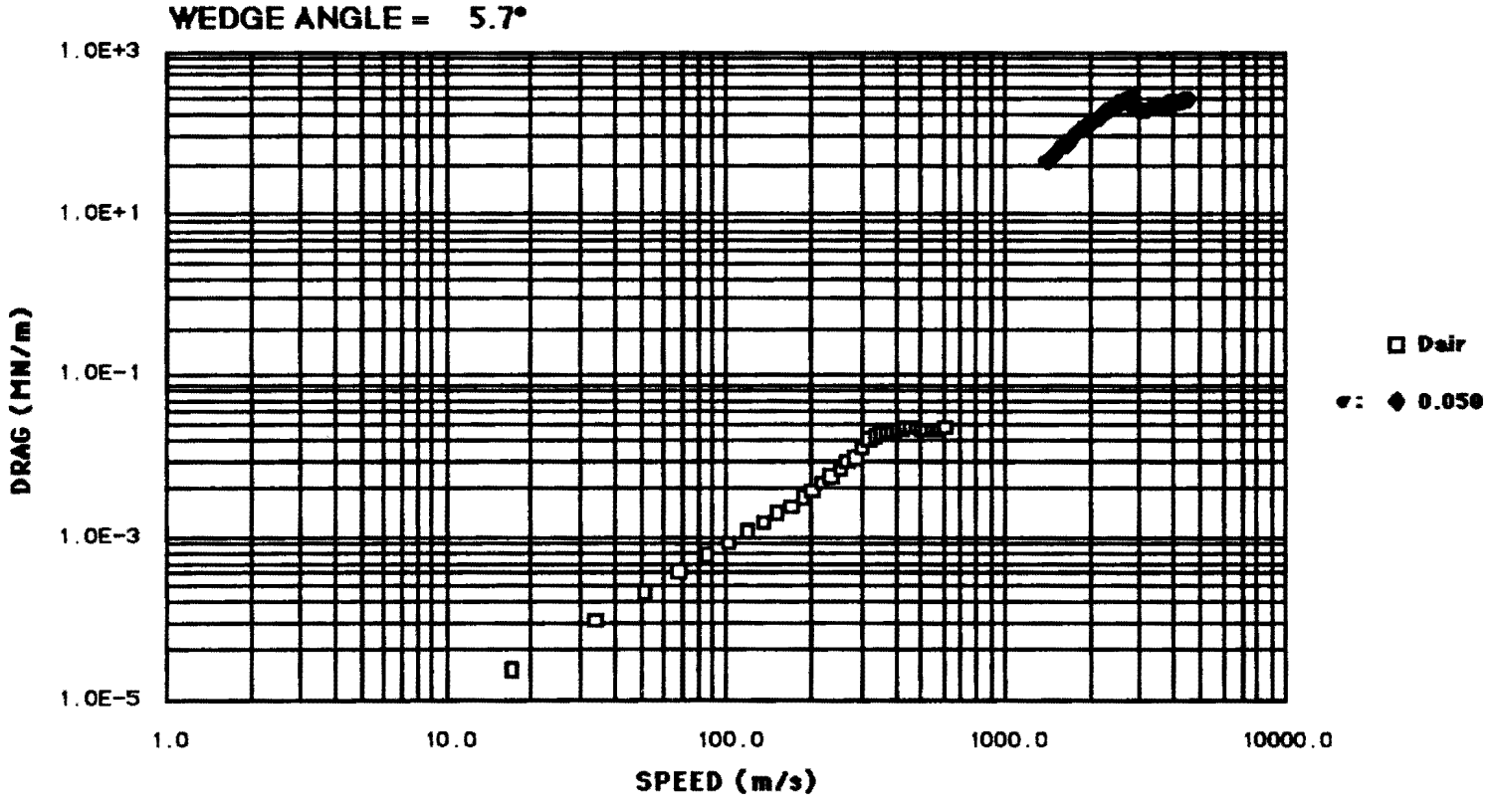

Figure 10. Estimates of Drag Forces in Air and Supercavitating in Water

CONCLUSIONS AND RECOMMENDATIONS

A review of supercavitation drag reduction in high-Mach-number liquid flows was performed in order to assess claims that experiments at such high speeds have been performed and to provide a comparison between the drag of projectiles traveling in water at transonic speeds versus the drag of similar projectiles in air at the same speed.

The physics of compressible flows was outlined in terms of the governing equations of motion, a comparison of the equations of state for air and water, the mechanics of shock and expansion waves for perfect gases, and the drag associated with a shock-wave system in the flow past a body.

Low-Mach-number supercavitation was briefly reviewed. A summary of results of a literature search concerning high-Mach-number supercavitating flows was presented, including a discussion of the various flow regimes of interest. Two papers of particular relevance were discovered (Nishiyama and Khan, 1981), and the key assumptions and results discussed.

The drag of bodies traveling at high-Mach numbers in air and supercavitating in water was discussed in more detail, with predictions made based on the Nishiyama-Khan model for a two-dimensional wedge at several values of the cavitation number. These results were compared with empirical data for the same wedge in air. Although the maximum values of the drag coefficient are within an order of magnitude over the range of cavitation numbers compared, the dimensional drag in water is much higher than that in air.

Assessment of Near-Mach-1 Undersea Claim

In spite of the high drag in water, there is no reason to disbelieve the claim of the Ukrainian scientist, Dr. Grimchenko because the range of the projectiles was not reported, but was certainly limited to the length of the test range, 100 m. The speed range of 1000 m/s to 1300 m/s probably covers the high-subsonic- through low-transonic regimes, depending on the cavitation number in the test tank.

Long-range propulsion of such vehicles would certainly be a challenge. Short-range gun launch, however, is subject to fewer constraints. These include the ability of the projectiles to withstand the launch without sustaining damage and the ability of the launcher to provide the impulse required to achieve the specified muzzle velocity.

Details of the launcher and projectile were not reported by Dr. Grimchenko, although the type of launcher was reported to be a hydrogen gun. Such a gun might be similar to a larger launcher used by the Lawrence Livermore National Laboratory and Rockwell in the development of supersonic combustion ramjets, often termed scramjets (Dornheim, 1993).

Experience with development of the AHSUM concept also indicates that directional stability at high speed requires careful projectile design. A variety of stabilizing mechanisms, including a series of fixed and pivoting noses, cavity-riding fins, and flared afterbodies, have been examined under the AHSUM program. It is not known what stabilizing mechanisms were employed by the Ukrainians in their high-Mach-number underwater tests.

Performance in Water Versus Performance in Air

The speed range of the empirical data reported in Hoerner (1965) for the in-air case does not reach the lower critical Mach number in water, even at the lowest cavitation number for which computations were performed. The in-air data could be extended using the theory from Ashley and Landahl (1965). Although this has not been done, it is quite apparent from the data shown in figure 10 that the drag in water greatly exceeds drag in air.

It is concluded that, contrary to previous speculation, the drag of high-Mach-number projectiles in water is much higher than the drag at the same speed in air. It appears that Dr. Seymour's statement, which seems to have been based solely on the ratio of the densities of water vapor to air, was oversimplified. It neglects the primary drag components of the high-Mach-number supercavitating case, including the base- and shock-wave drag components.

In fairness to Dr. Seymour, it is suspected that his comments were reported out of context. A complete and accurate drag prediction for either the in-air case or the case of supercavitation at high-Mach numbers in water is beyond even the scope of many sophisticated computational tools. The flow case reported at the NSF symposium does not fall within the experience of most scientists, and casual comment and speculation should not be judged too harshly: The imagination of most knowledgeable people would be similarly stimulated by such a report.

Supercavitation As a Drag-Reduction Technique

Under certain conditions, substantial drag reduction can be achieved through the use of passive body supercavitation, even at high-Mach numbers, provided the body is designed to take advantage of the cavity shape. The proper figure of merit for such designs involves the total dimensional drag and the useful vehicle volume.

Although not extensively studied, high-Mach-number supercavitating flows are tractable for prediction using a combination of standard techniques. Experimental verification, however, will be a challenge. Additionally, some aspects of the flow topology (that is, the various shock- and expansion wave structures occurring in the flow and their relationship to separation bubbles and cavities) are not well understood.

Recommendations

A more complete validation of the Nishiyama-Khan model is required. Possibilities for simple experimental verification of such high-Mach-number supercavitation models should be explored. As the AHSUM program results in projectiles of increasingly higher speed, pertinent data will become available.

Until experimental data become available, validation could be initiated by comparing results of the Nishiyama-Khan model with those of other computations. New development of the marker-in-cell technique (Johnson, et al, 1994) and the discrete vortex element (DVE) method (Huyer, et al, 1994) might be well-suited to such investigation.

Provided its validity can be assured, the Nishiyama-Khan model should be extended to more complicated shapes, to axisymmetric and three-dimensional flows, and to an analysis similar to that above perform for axisymmetric shapes representative of practical undersea missiles.

Finally, it should be noted that a simple problem can be formulated for deducing optimal trajectories for both low- and high-Mach-number supercavitating bodies. In such a problem, the depths of the launcher and the target would be specified, along with some estimated functional relationship between drag, speed, and depth. A variety of standard techniques exist for determining the trajectory that minimizes either the time to target-strike or the total power consumed. Such an investigation might provide useful information concerning deployment of weapons employing supercavitation drag reduction.

It is recommended that the Office of Naval Intelligence encourage the Office of Naval Research to fund additional research in these areas.

BIBLIOGRAPHY

Ashley, H., and M. Landahl (1965), *Aerodynamics of Wings and Bodies,* Dover Publications, Inc., New York.

Chou, Y.S. (1974), "Axisymmetric Cavity Flows Past Slender Bodies of Revolution," *Journal of Hydronautics*, vol. 8, no. 1.

Dornheim, M.A. (1993), "Livermore Gun Fires Scramjet at Mach 8," *Aviation Week & Space Technology* , December 13-20.

Hickox, C.E., C.E. Hailey, W.P. Wolfe, H.A. Watts, R.J. Gross, and M.S. Ingber (1988), "Numerical Description of Cavitation on Axisymmetric Bodies," Sandia National Laboratories.

Hirt, C.W. (1990), "Computational Modeling of Cavitation," Flow Science, Inc., Los Alamos, NM.

Hoerner, S.F. (1965), *Fluid-Dynamic Drag,* Hoerner Fluid Dynamics, Brick Town, NJ.

Huyer, S.A., J.R. Grant, and J.S. Uhlman (1994), "A Vortex Element Representation of Two-Dimensional Unsteady Separated Flow Fields," *Proceedings of the 32nd Aerospace Sciences Meeting & Exhibit,* Reno, NV, January 10-13.

Johnson, D.B., P.E. Raad, and S. Chen (1994), "Simulation of Impacts of Fluid Free Surfaces with Solid Boundaries," accepted for publication *International Journal of Numerical Meth Fluids.*

Kirschner, I.N. (1993), "Adaptable High-Speed Undersea Missile for Mine Neutralization," *6th Annual NUWC IR&D Symposium and ADPA USW Divsion Annual Fall Meeting.*

Kochendorfer, P.M. (1993), "High-Velocity Underwater Projectile Demonstration Test Plan," Technical Report PDA-93-TR-1722-00-03; PDA Engineering, Costa Mesa, CA.

Meng, J.C-S., I.N. Kirschner, J.Q. Rice, C.J. Egan, and W.L. Harbison (1994), "Engineering, Physics, and Assessment of Supercavitating Drag Reduction for a High-Speed Underwater Vehicle," NUWC-NPT TR. (awaiting final publication).

Meng, J.C-S., J.Q. Rice, I.N. Kirschner, W.L. Harbison, and C.J. Egan (1992a), "High-Speed Underwater Missile," presented to NAVMIC (Mssrs. K. Parys, T. Kelly, and S. Tagg).

Meng, J.C-S., W.H. Wilson, R.L. Schmidt, I.N. Kirschner, J.Q. Rice, W.L. Harbison, and C.J. Egan (1992b), "High-Speed Underwater Missile," presented to ONT (Dr. P.A. Selwyn).

"Ukrainians approach Mach-1 Speeds Under Water," (1993), *Navy News & Undersea Technology* vol. 10 1, no. 1.

Newman, J.N. (1980), *Marine Hydrodynamics,* The MIT Press, Cambridge, MA.

Nishiyama, T. and O.F. Khan (1981a), "Compressibility Effects Upon Cavitation in High-Speed Liquid Flow (first report: "Subsonic Liquid Flow"), *Bulletin of the Japanese Society of Mechenical Engineers* vol. 24, 190.

Nishiyama, T. and O.F. Khan (1981b), "Compressibility Effects Upon Cavitation in High-Speed Liquid Flow (second report: "Transonic and Supersonic Liquid Flows"), *Bulletin of the Japanese Society of Mechenical Engineers* vol. 24 190.

Oberkampf, W.L. and W.P. Wolfe (1986), "Drag of Bodies of Revolution in Cavitating Flow," *AIAA/ASME 4th Fluid Mechanics, Plasma Dynamics, and Lasers Conference.*

Pai, S.I. and L. Shijun (1991), *Theoretical and Computational Dynamics of a Compressible Flow,* Van Nostrand Reinhold, New York.

Shapiro, A.H. (1953), *The Dynamics and Thermodynamics of Compressible Fluid Flow,* The Ronald Press Company, New York.

Streeter, V.L., ed. (1961), *Handbook of Fluid Dynamics,* McGraw-Hill, New York.

Sutton, G.P. (1956), *Rocket Propulsion Elements,* John Wiley & Sons, Inc., New York.

Van Dyke, M. (1982), *An Album of Fluid Motion,* Parabolic Press, Stanford, CA.

Vorus, W.S. (1986), "Ambient Supercavities of Slender Bodies of Revolution," *J Ship Res* , vol. 30 no. 3.

Vorus, W.S. (1991), "A Theoretical Study of the Use of Supercavitation/Ventilation for Underwater Body Drag Reduction," Vorus & Associates.

Wu, T.Y. (1976), "Cavity Flow and Numerical Methods," *1st International Conference on Numerical Ship Hydrodynamics.*

Zucrow, M.J. and J.D. Hoffman (1976), *Gas Dynamics,* vol. 1, John Wiley & Sons, Inc., New York.

DISTRIBUTION LIST

External

Chief of Naval Operations (Code N2--S. Tagg (2))
Office of Naval Research (J. Fein, K. Latt, P. Purtell, E. Rood, S. Lekoudis)
PDA Engineering (P. Kochendorfer)
Southern Methodist University (P. Raad)
University of Michigan (W. Vorus)

Internal

Codes:
01
02244
0251 (Conforti)
0261 (NLON Library)
0262 (NPT Library (2))
10
102 (K. Lima)
104
106 (S. Dickinson)
20
2141 (W. Keith)
22
38
382
383
423 (C. Wagner)
60
6292
72
80 (B. Myers)
81
814
82
8219 (R. Schmidt)
823
8231 (J. Hrubes)
8233
8233 (P. Bandyopadhyay, J. Grant, S. Huyer, I. Kirschner (5), J. Rice (2), A. Varghese (2))
8291 (C. Egan)
83
8311
832
8322
8322 (J. Cipolla)
833

Total: 57